Supplement of Atmos. Chem. Phys., 24, 2423–2441, 2024
https://doi.org/10.5194/acp-24-2423-2024-supplement

Atmospheric Chemistry and Physics
Open Access
EGU

Supplement of

Elucidating the mechanisms of atmospheric new particle formation in the highly polluted Po Valley, Italy

Jing Cai et al.

Correspondence to: Dominik Stolzenburg (dominik.stolzenburg@tuwien.ac.at) and Federico Bianchi (federico.bianchi@helsinki.fi)

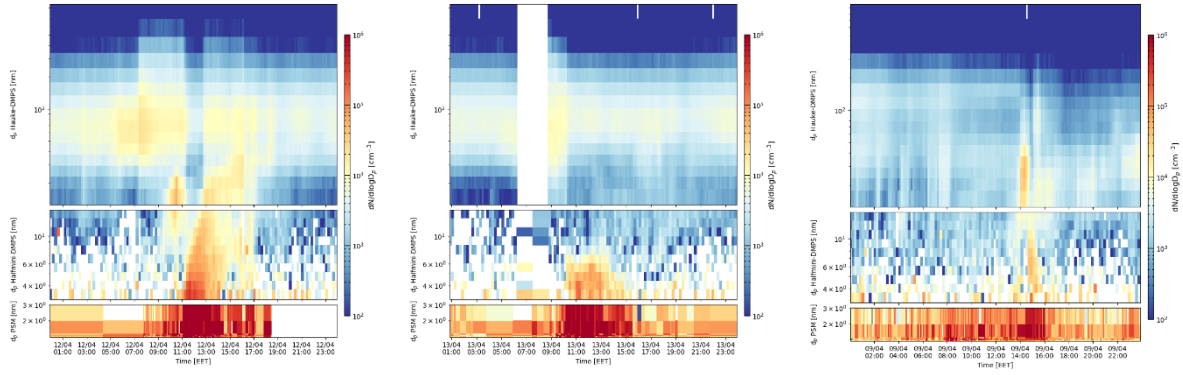

Figure S1. Particle size distributions (x-axis time, y-axis size in nm and color code is number concentration in dN/dlogDp) from 1.3 – 800 nm as measured by three different instruments (upper panel Hauke-DMPS, middle panel Halfmini-DMPS and lower panel PSM) for a) an NPF with growth event (12th of April), b) an NPF with growth event and c) a non-NPF day.

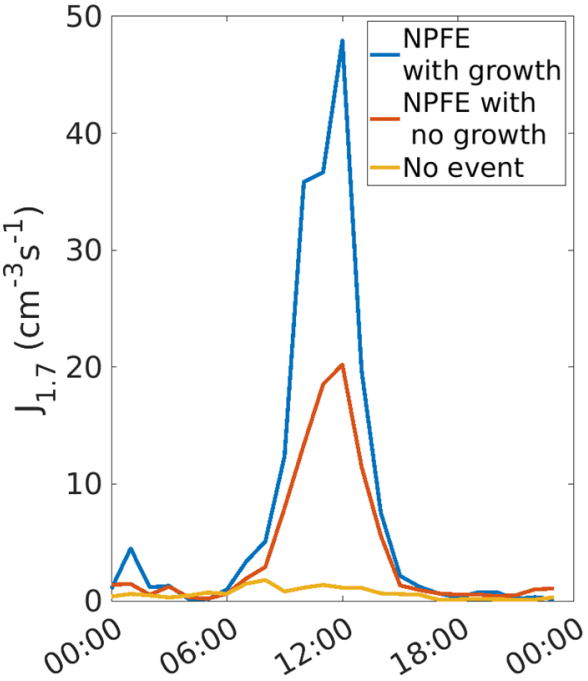

Figure S2. The formation rate of 1.7 nm particles ($J_{1.7}$) during NPF with growth, NPF without growth and no NPF events during our sampling period.

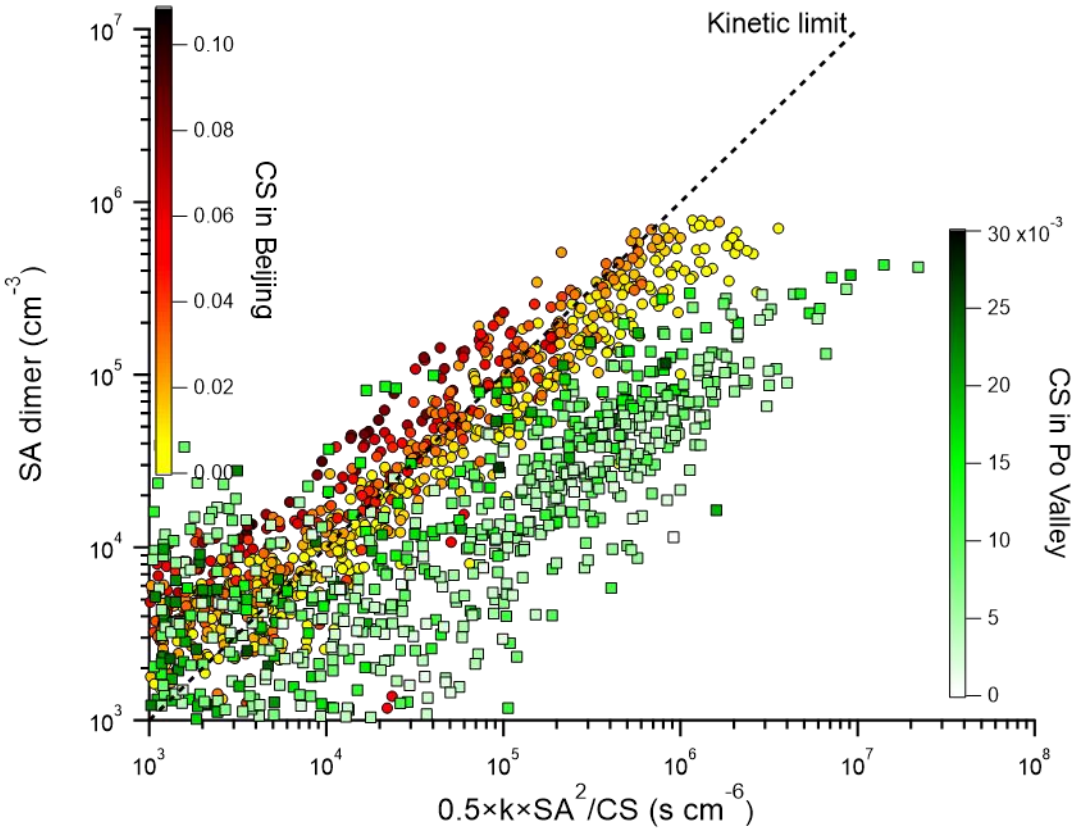

Figure S3. The relationship between sulfuric acid dimer concentration (SA dimer), monomer concentration (SA), and the CS in the Po Valley region. The theoretical molecular collision rate constant (k) was set as 4×10^{-10} cm^3 s^{-1} (Stolzenburg et al., 2020).

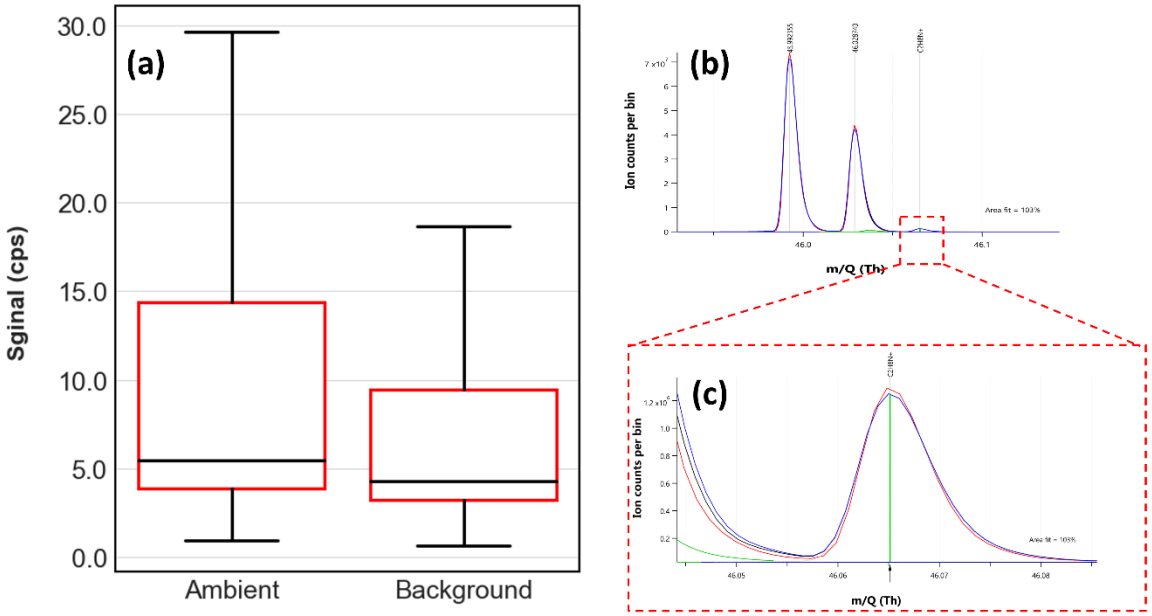

Figure S4. (a) C_2H_7N signal observed from March to April (excluding outliers). (b) Peak fitting at m/z 46. (c) Zoomed-in view of $C_2H_8N^+$ (DMA) peak fitting.

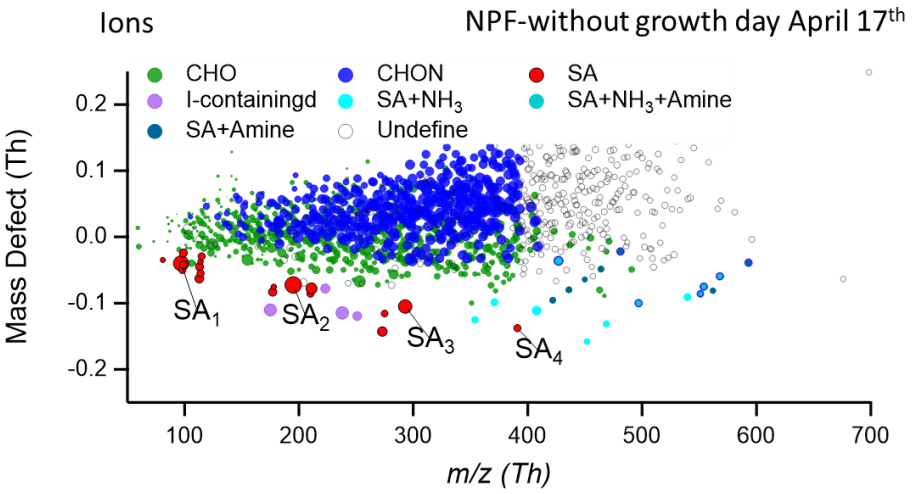

Figure S5. Mass defect plots for ion clusters during the NPF without growth day (10:00 − 14:00 of April 17th). The size of the dots is proportional to the logarithm of the signal intensity of each cluster.

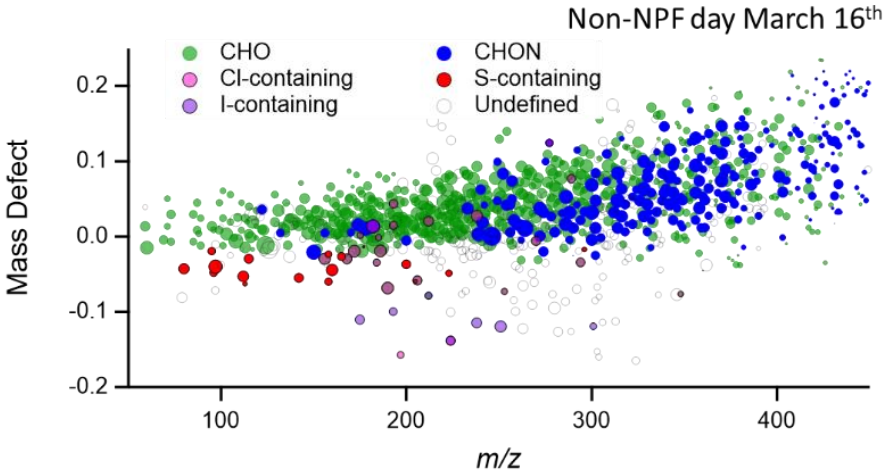

Figure S6. Mass defect plots for neutral clusters during the non NPF period (10:00 − 14:00 of March 16th). The size of the dots is proportional to the logarithm of the signal intensity of each cluster.

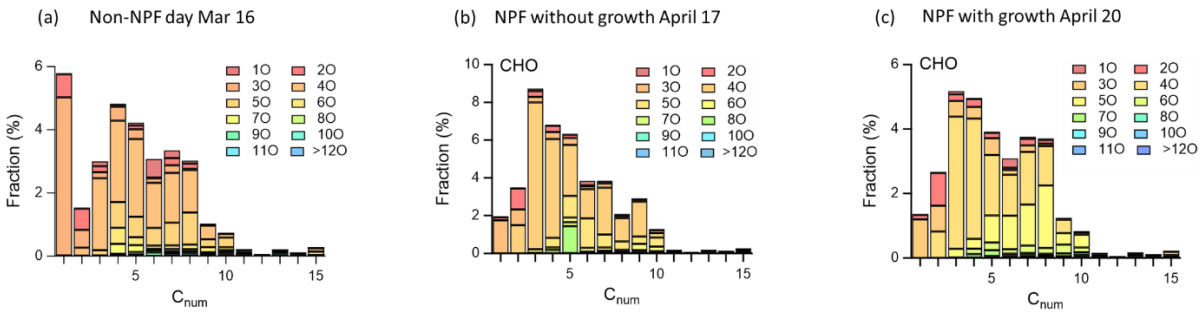

Figure S7. Signal fractions to total identified organic molecules with different numbers of oxygen and carbon atoms of CHO compounds in the (a) non-NPF day (March 16), (b) NPF with no growth day (April 17) and NPF with growth day (April 20) during peak hours (10:00 – 14:00).

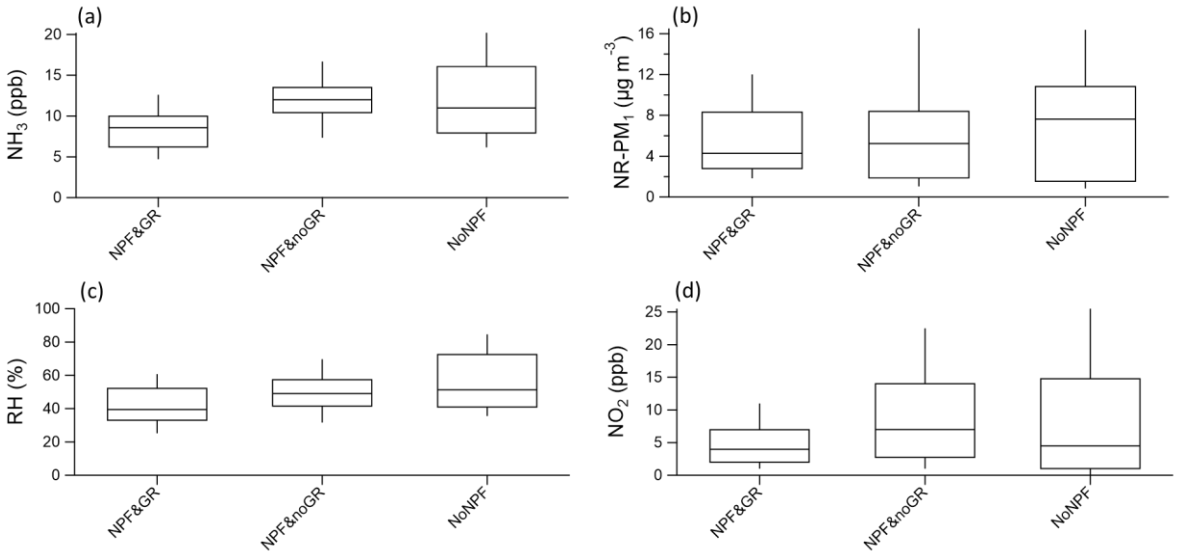

Figure S8. (a) the NH_3, (b) NR-PM_1, (c) RH, and (d) NO_2 for NPF with growth (NPF&GR), NPF without growth (NPF&noGR) and no NPF event (NoNPF) days. In each box plot, the median (middle horizontal line), 25th and 75th percentiles (bottom and top ends of the box, respectively), and 10th and 90th percentiles (bottom and top whiskers, respectively) are presented.

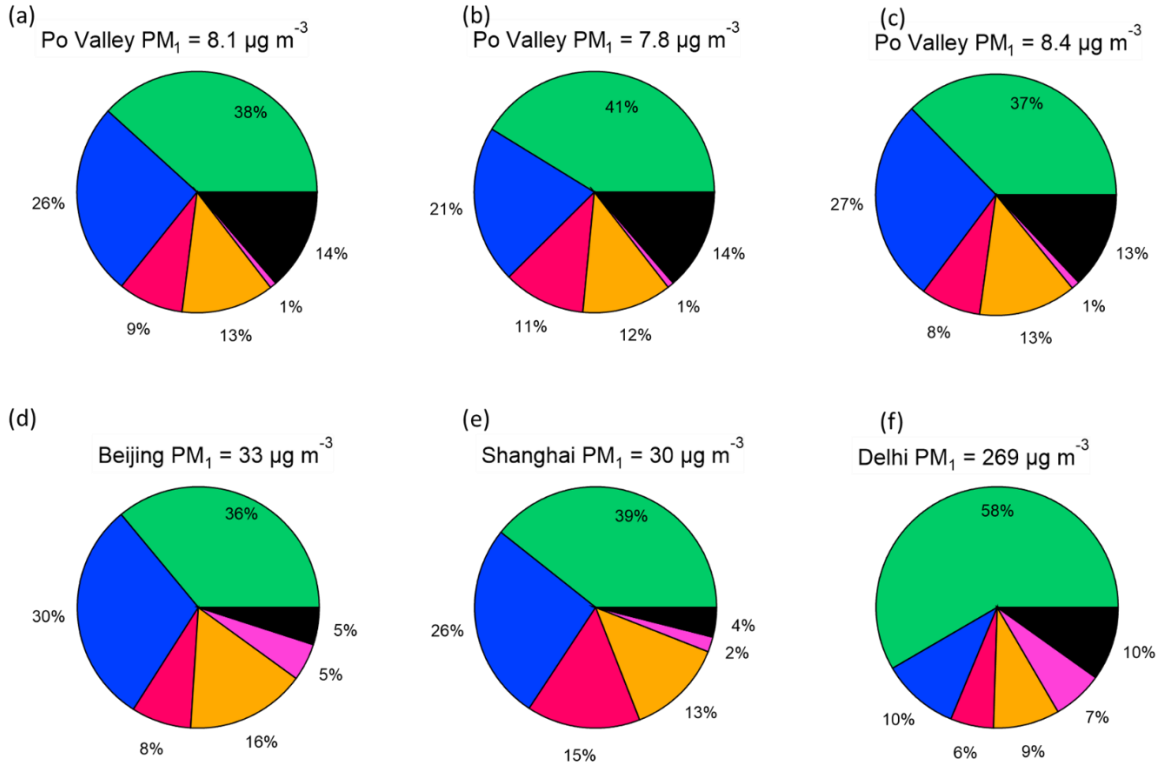

Figure S9. The comparison of PM_1 compositions between Po Valley and other polluted cities. PM_1 compositions in (a) Po Valley for all days, (b) Po Valley for NPF with growth days, (c) Po Valley for non-NPF days, (d) Beijing, (e) Shanghai, (f) Delhi. The green, blue, red, orange, chloride and black colors represented organics, nitrate, sulfate, ammonium, chloride, and BC, respectively. The NR-PM_1 is from a co-located aerosol mass spectrometer measurement (Paglione et al., 2020) and BC concentration is from the MAAP measurement with $PM_{2.5}$ inlet. The

chemical compositions of Beijing (Li et al., 2019), Shanghai (Song et al., 2023), and Delhi (Mishra et al., 2023) are from previous literature.

Table S1. Ambient NH_3 and DMA concentrations from different measurement sites

Site	Sampling period	DMA (ppt)	NH_3 (ppb)	Instrument	Ref
Beijing	Oct 2018- Nov 2018	7.3	20.8	H_3O^+-tof-CIMS	Cai et al., 2021
Wangdu	Dec 2018-Jan 2019	14.6	31.2	Vocus	Wang et al., 2020
Shanghai	Jul 2015-Aug 2015	40	9.3	Protonated ethanol-CIMS	Yao et al., 2016
Nanjing	Sep 2022-Oct 2022	20.8	13.1	Vocus (DMA), Picarro (NH_3)	unpublished data
Hyytiälä	Mar-Dec 2015	< LOD	0.066	MARGA (both DMA and NH_3)	Hemmilä et al., 2018
Po Valley	Mar 2022-May 2022	Not quantified	10.6	Vocus (DMA)	this study

Note: The Limit of Detection (LOD) for DMA with instrument for Measuring AeRosols and Gases in Ambient Air (MARGA) is 1.7 ppt and the LOD for DMA with Vocus is 1.44 ppt

Reference

Li, H., Cheng, J., Zhang, Q., Zheng, B., Zhang, Y., Zheng, G., and He, K.: Rapid transition in winter aerosol composition in Beijing from 2014 to 2017: response to clean air actions, Atmospheric Chemistry and Physics, 19, 11485-11499, 10.5194/acp-19-11485-2019, 2019.

Mishra, S., Tripathi, S. N., Kanawade, V. P., Haslett, S. L., Dada, L., Ciarelli, G., Kumar, V., Singh, A., Bhattu, D., Rastogi, N., Daellenbach, K. R., Ganguly, D., Gargava, P., Slowik, J. G., Kulmala, M., Mohr, C., El-Haddad, I., and Prevot, A. S. H.: Rapid night-time nanoparticle growth in Delhi driven by biomass-burning emissions, Nature Geoscience, 16, 224-230, 10.1038/s41561-023-01138-x, 2023.

Paglione, M., Gilardoni, S., Rinaldi, M., Decesari, S., Zanca, N., Sandrini, S., Giulianelli, L., Bacco, D., Ferrari, S., Poluzzi, V., Scotto, F., Trentini, A., Poulain, L., Herrmann, H., Wiedensohler, A., Canonaco, F., Prévôt, A. S. H., Massoli, P., Carbone, C., Facchini, M. C., and Fuzzi, S.: The impact of biomass burning and aqueous-phase processing on air quality: a multi-year source apportionment study in the Po Valley, Italy, Atmospheric Chemistry and Physics, 20, 1233-1254, 10.5194/acp-20-1233-2020, 2020.

Song, Z., Gao, W., Shen, H., Jin, Y., Zhang, C., Luo, H., Pan, L., Yao, B., Zhang, Y., Huo, J., Sun, Y., Yu, D., Chen, H., Chen, J., Duan, Y., Zhao, D., and Xu, J.: Roles of Regional Transport and Vertical Mixing in Aerosol Pollution in Shanghai Over the COVID‐19 Lockdown Period Observed Above Urban Canopy, Journal of Geophysical Research: Atmospheres, 128, 10.1029/2023jd038540, 2023.

Stolzenburg, D., Simon, M., Ranjithkumar, A., Kürten, A., Lehtipalo, K., Gordon, H., Ehrhart, S., Finkenzeller, H., Pichelstorfer, L., Nieminen, T., He, X.-C., Brilke, S., Xiao, M., Amorim, A., Baalbaki, R., Baccarini, A., Beck, L., Bräkling, S., Caudillo Murillo, L., Chen, D., Chu, B., Dada, L., Dias, A., Dommen, J., Duplissy, J., El Haddad, I., Fischer, L., Gonzalez Carracedo, L., Heinritzi, M., Kim, C., Koenig, T. K., Kong, W., Lamkaddam, H., Lee, C. P., Leiminger, M., Li, Z., Makhmutov, V., Manninen, H. E., Marie, G., Marten, R., Müller, T., Nie, W., Partoll, E., Petäjä, T., Pfeifer, J., Philippov, M., Rissanen, M. P., Rörup, B., Schobesberger, S., Schuchmann, S., Shen, J., Sipilä, M., Steiner, G., Stozhkov, Y., Tauber, C., Tham, Y. J., Tomé, A., Vazquez-Pufleau, M., Wagner, A. C., Wang, M., Wang, Y., Weber, S. K., Wimmer, D., Wlasits, P. J., Wu, Y., Ye, Q., Zauner-Wieczorek, M., Baltensperger, U., Carslaw, K. S., Curtius, J., Donahue, N. M., Flagan, R. C., Hansel, A., Kulmala, M., Lelieveld, J., Volkamer, R., Kirkby, J., and Winkler, P. M.: Enhanced growth rate of atmospheric particles from sulfuric acid, Atmospheric Chemistry and Physics, 20, 7359-7372, 10.5194/acp-20-7359-2020, 2020.